

Drawing Multiple Augmentation Samples Per Image During Training Efficiently Decreases Test Error

Stanislav Fort *
Stanford University
sfort1@stanford.edu

Andrew Brock
DeepMind
ajbrock@deepmind.com

Razvan Pascanu
DeepMind
razp@deepmind.com

Soham De
DeepMind
sohamde@deepmind.com

Samuel L. Smith
DeepMind
slsmith@deepmind.com

Abstract

In computer vision, it is standard practice to draw a single sample from the data augmentation procedure for each unique image in the mini-batch, however it is not clear whether this choice is optimal for generalization. In this work, we provide a detailed empirical evaluation of how the number of augmentation samples per unique image influences performance on held out data. Remarkably, we find that drawing multiple samples per image consistently enhances the test accuracy achieved for both small and large batch training, despite reducing the number of unique training examples in each mini-batch. This benefit arises even when different augmentation multiplicities perform the same number of parameter updates and gradient evaluations. Our results suggest that, although the variance in the gradient estimate arising from subsampling the dataset has an implicit regularization benefit, the variance which arises from the data augmentation process harms test accuracy. By applying augmentation multiplicity to the recently proposed NFNet model family, we achieve a new ImageNet state of the art of 86.8% top-1 w/o extra data.

1 Introduction

Data augmentation plays a crucial role in computer vision, and it is currently essential to achieve competitive performance on held-out data [Shorten and Khoshgoftaar, 2019]. However the origin of the benefits of data augmentation are not fully understood. In addition, a number of authors have identified that SGD has an implicit regularization benefit, whereby large learning rates and small batch sizes achieve higher accuracy on held-out data [Keskar et al., 2017, Mandt et al., 2017, Smith and Le, 2018, Jastrzebski et al., 2018, Chaudhari and Soatto, 2018, Li et al., 2019, Smith et al., 2021], yet most authors have not considered how data augmentation and SGD interact during training.

In this work, we note that data augmentation has two distinct influences on the gradient of a single training example. First, augmentation operations like left-right flips, random crops or RandAugment [Cubuk et al., 2020] change the expected value of the gradient of an example, introducing bias. Second, since we draw a finite number of samples from the augmentation procedure in each mini-batch (typically one per unique image), data augmentation also introduces variance to the gradient. A key goal of this work is to establish whether the benefits of data augmentation arise solely from bias, or whether the variance introduced by the augmentation procedure is also beneficial [Wei et al., 2020]. In addition, we wish to understand how the variance introduced by the augmentation procedure interacts with the variance introduced when we estimate the gradient on a subset of the training set.

*Work performed while interning at DeepMind.

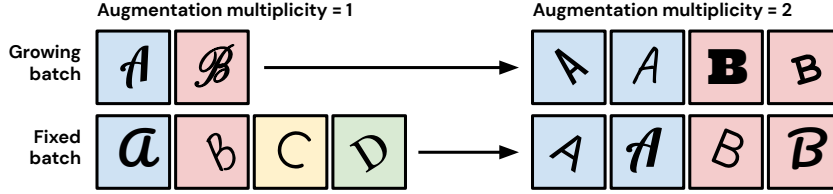


Figure 1: Two forms of augmentation multiplicity. In the top row we draw 2 augmentation samples per image, while preserving the number of unique examples in the batch (‘growing batch’). In the bottom row we draw 2 augmentation samples per image, but hold the batch size fixed (‘fixed batch’).

To achieve this, we exploit a simple modification to the standard training pipeline; augmentation multiplicity (see Figure 1) [Hoffer et al., 2019, Choi et al., 2019]. The key insight of augmentation multiplicity is that we can preserve the bias in the per-example gradients introduced by data augmentation, while simultaneously suppressing the variance, by drawing multiple augmentation samples of each unique image in the mini-batch. One can achieve this either by allowing the batch size to grow as the multiplicity increases, or by reducing the number of unique examples in each mini-batch. We study both schemes in this work. Since SGD exhibits different behaviour at different batch sizes [Goyal et al., 2017, Ma et al., 2018, Zhang et al., 2019, Smith et al., 2020], we also study augmentation multiplicity in both the small and large batch regimes. Our key findings are as follows:

1. When the number of unique images per batch is fixed (the batch size grows as the augmentation multiplicity increases) the test accuracy rises as the augmentation multiplicity rises. This phenomenon arises even after we tune the epoch budget, which suggests the benefits of data augmentation arise from the bias in the gradient, not the variance. Note that by contrast, performance degrades for very large batch sizes in standard pipelines [Smith et al., 2020].
2. In addition, augmentation multiplicities greater than 1 continue to achieve higher test accuracy, even if we hold the total batch size fixed, such that the number of unique images per batch decreases. This benefit is particularly pronounced for large batch training, but it also arises for small batch sizes. In this setting, despite their superior performance on the test set, large augmentation multiplicities achieve slower convergence on the training set.
3. We provide an empirical evaluation of augmentation multiplicity on NFNet [Brock et al., 2021b]. Using an NFNet-F5 with SAM regularization and augmentation multiplicity 16 at batch size 4096, we set a new ImageNet SOTA of 86.8% top-1 w/o extra data. We achieve this result after training for 34 epochs (168900 steps), while the previous SOTA was set by a larger model trained for 360 epochs (112600 steps). Our results demonstrate that most computation used when training NFNet simply reduces the variance of data augmentation.
4. To explain our observations, we note that when the batch size is fixed, large augmentation multiplicities increase the overall variance in the minibatch gradient estimate, since the number of unique images in each batch is reduced. However because we draw multiple samples of the augmentation procedure for each image, the variance in the per-example gradients is reduced. We conclude that the variance in the gradient estimate arising from sub-sampling the dataset has an implicit regularization benefit enhancing generalization, while the variance arising from the data augmentation procedure harms test accuracy.

Augmentation multiplicity was first proposed in an empirical study by Hoffer et al. [2019] as a promising strategy for large batch training, while Choi et al. [2019] explored using augmentation multiplicity to reduce communication overheads on device. Augmentation multiplicity was also recently used by Touvron et al. [2021] to enhance the performance of vision transformers [Dosovitskiy et al., 2020]. In this work, we provide the first systematic study of how augmentation multiplicity influences deep networks trained with SGD in a range of different regimes, and we seek to explain why large augmentation multiplicities enhance generalization. We find that large augmentation multiplicities achieve higher test accuracy for both small and large batch sizes, and crucially they can exceed state of the art performance without requiring larger compute budgets. We therefore believe large augmentation multiplicities should become the default setting in many vision applications.

This paper is structured as follows. In Section 2, we evaluate the performance of augmentation multiplicity when the number of unique images per batch is fixed. This section demonstrates that the

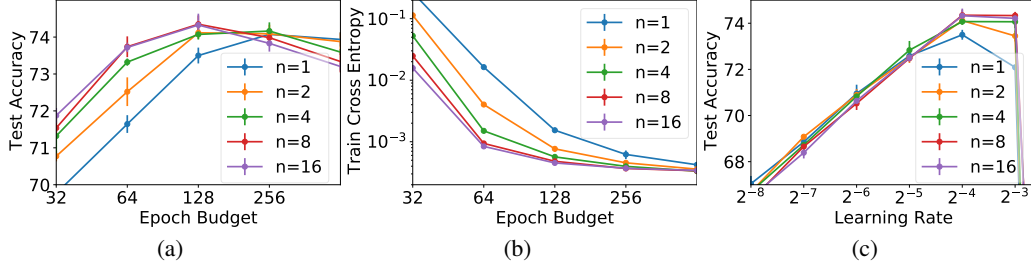


Figure 2: Results with a 16-4 Wide-ResNet on CIFAR-100. The number of unique images per batch is fixed, such that the batch size grows as the augmentation multiplicity n increases. (a) Test accuracies at optimal learning rates for a range of epoch budgets. Large augmentation multiplicities achieve higher overall test accuracies, and also require fewer training epochs. (b) The training cross entropy for a range of epoch budgets. In this growing batch setting, large augmentation multiplicities achieve smaller training losses. (c) The test accuracy at a range of learning rates for a compute budget of 128 epochs. Different augmentation multiplicities achieve similar test accuracy when the learning rate is small, but large augmentation multiplicities achieve higher test accuracy with large learning rates.

variance introduced by the augmentation procedure harms test accuracy. In Section 3 we evaluate the performance of augmentation multiplicity when the total batch size is fixed, to demonstrate that augmentation multiplicity is a practical method for enhancing model performance with limited hardware. We discuss why augmentation multiplicity enhances generalization in Section 4. Finally, we apply augmentation multiplicity to the NFNets model family [Brock et al., 2021b] in Section 5.

2 The benefits of data augmentation arise from bias, not variance

In this section, we show that the primary benefits of data augmentation in ResNets arise from the bias in the augmentation procedure, not the variance. We consider a 16-4 Wide-ResNet [Zagoruyko and Komodakis, 2016], trained on CIFAR-100 [Krizhevsky et al., 2009] with padding, left-right flips and random crops. The data augmentation process introduces a bias in the evaluated gradients. More specifically, if $\ell(x)$ denotes the loss for input x and $F(x, \xi)$ denotes the augmentation function whose output is the augmented image, with ξ being the collection of random variables denoting the noise in the augmentation process, then data augmentation changes the expected value of the loss since:

$$\mathbb{E}_{\xi}[\ell(F(x, \xi))] \neq \ell(x). \quad (1)$$

However, typically practitioners only augment each image in a mini-batch once by sampling a single ξ_1 and computing $\ell(F(x, \xi_1))$. This introduces additional variance in the training process. To disentangle the effects of bias and variance on final model performance, we train with a range of augmentation multiplicities n , meaning that for each unique input x , we produce n augmented inputs by drawing n random samples of the noise ξ , and average the loss over these n samples:

$$\frac{1}{n} \sum_{i=1}^n \ell(F(x, \xi_i)). \quad (2)$$

Larger augmentation multiplicities reduce the gradient covariance, helping to isolate the effect of the bias. In all the experiments shown in this section, we draw 64 unique inputs in each minibatch, such that the total batch size $B = 64n$ grows with the augmentation multiplicity. By keeping the number of unique examples in the minibatch fixed, we ensure that we isolate the role of the variance in the data augmentation procedure, without increasing the variance arising from sub-sampling the dataset.

The performance of batch-normalized networks depends strongly on the examples used to evaluate the batch statistics [Hoffer et al., 2017]. In the main text, we therefore train without normalization using the SkipInit initialization scheme [De and Smith, 2020]. We provide additional experiments with batch normalization in appendix A, for which we observe similar behaviour. We use SGD with a momentum coefficient of 0.9 and weight decay with a coefficient of 5×10^{-4} . When training for m epochs, the learning rate is constant for the first $m/2$ epochs, and then decays by a factor of 2 every remaining $\frac{m}{20}$ epochs. We provide the mean accuracy of the best 5 out of 7 training runs.

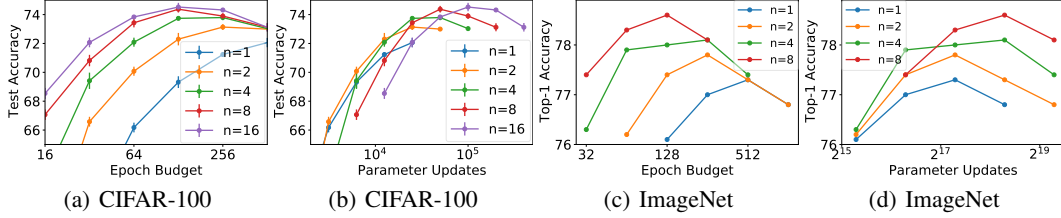


Figure 3: Large augmentation multiplicities achieve significantly higher test accuracy for large batch training. Here the batch size is independent of the augmentation multiplicity n , such that the number of unique images per batch declines as the multiplicity increases. Note large multiplicities perform more parameter updates per epoch. We show the test accuracy achieved for a given epoch budget (a/c) and for a given number of parameter updates (b/d). Figures a and b consider a 16-4 Wide-ResNet trained on CIFAR-100 at batch size 1024, while figures c and d consider an NF-ResNet50 trained on ImageNet at batch size 4096. In both cases, large augmentation multiplicities achieve substantially higher test accuracy, requiring fewer training epochs and without requiring more parameter updates.

In Figure 2(a), we plot the test accuracy for a range of augmentation multiplicities. Since large multiplicities perform more gradient evaluations per minibatch, we also evaluate the performance across a range of epoch budgets. Note that we independently tune the learning rate on a logarithmic grid spaced by factors of 2 for each combination of epoch budget and augmentation multiplicity. After tuning the epoch budget, we find that large augmentation multiplicities achieve slightly higher test accuracy. For instance, augmentation multiplicity 16 achieves a peak test accuracy of $74.3 \pm 0.1\%$ after 128 epochs, while augmentation multiplicity 1 (normal training) achieves a peak of $74.1 \pm 0.01\%$ after 256 epochs. Since higher augmentation multiplicities reduce the variance from data augmentation without changing the bias, this confirms that the variance arising from data augmentation reduces the test accuracy. Large augmentation multiplicities also require fewer training epochs/parameter updates to reach optimal performance, indicating that the variance slows down training. Intriguingly, large augmentation multiplicities do achieve lower test accuracy when the epoch budget is very large, suggesting the variance from the augmentation procedure can help prevent over-fitting when models are over-trained. For completeness, we note that training without data augmentation at batch size 64 achieves a substantially lower test accuracy of 61.4% after tuning both the learning rate and compute budget, verifying that the bias introduced by data augmentation significantly enhances generalization. We provide additional results in Appendix B on ImageNet [Russakovsky et al., 2015] for a ResNet-50 [He et al., 2016] with 256 unique images per batch, trained using the Norm-Free (NF-) scheme of Brock et al. [2021a], for which large augmentation multiplicities also achieve higher test accuracy.

In Figure 2(b), we demonstrate that large augmentation multiplicities also achieve faster convergence on the training set in this “growing batch” setting. This is intuitive, since large multiplicities perform more gradient evaluations per minibatch, reducing the variance of the gradient estimate. For clarity, we plot the training loss at the learning rate in our grid which minimizes the training loss. We evaluate the training loss on the full training dataset using the raw images (without data augmentation).

Finally in Figure 2(c), we plot how the test accuracy for a budget of 128 epochs depends on the learning rate. Note that 128 epochs is the optimal epoch budget for large augmentation multiplicities. We find that different multiplicities achieve similar test accuracy when the learning rate is small, but large augmentation multiplicities achieve higher test accuracy when the learning rate is large, and this enables large augmentation multiplicities to achieve higher overall test accuracy after tuning. These results suggest that the variance in the data augmentation operation reduces the stability of training, which impairs training with large learning rates and consequently reduces test performance [Smith et al., 2021]. We discuss the role of large learning rates for generalization in more detail in Section 4.

3 An empirical evaluation of augmentation multiplicity for fixed batch sizes

In Section 2 we established that for Wide-ResNets, the benefits of data augmentation arise from the bias in the gradient estimate, not the variance. In addition, we showed large augmentation multiplicities can achieve higher test accuracy, even after tuning the compute budget. However we allowed the minibatch size to grow as the augmentation multiplicity rose. This is impractical, since the batch size is usually determined by the hardware available for training. In this section, we confirm

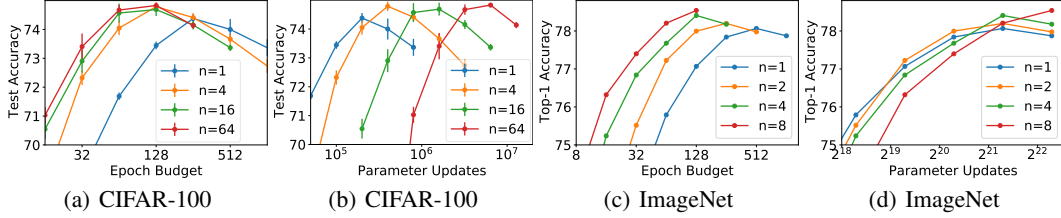


Figure 4: Large augmentation multiplicities also achieve higher test accuracy for small batch training. We show the test accuracy achieved for a given epoch budget (a/c) and for a given number of parameter updates (b/d). Figures a and b consider a 16-4 Wide-ResNet trained on CIFAR-100 with a fixed batch size of 64, while figures c and d consider an NF-ResNet50 trained on ImageNet with a fixed batch size of 256. In both cases augmentation multiplicities greater than 1 achieve higher test accuracy in fewer training epochs while requiring similar or slightly larger numbers of parameter updates.

that large augmentation multiplicities continue to achieve superior test accuracy if we maintain a constant batch size B , such that the number of unique training examples per minibatch declines as the augmentation multiplicity increases [Touvron et al., 2021]. The behaviour of SGD differs substantially in the small batch, ‘noise dominated’ regime and the large batch, ‘curvature dominated’ regime [Zhang et al., 2019, Smith et al., 2020]. We therefore consider both regimes separately here.

We consider two models; A 16-4 Wide-ResNet trained on CIFAR-100 at batch sizes 64 (small) and 1024 (large), and an NF-ResNet-50 [Brock et al., 2021a] trained on ImageNet at batch sizes 256 (small) and 4096 (large). We described the Wide-ResNet model and CIFAR-100 training pipeline in section 2. We train the NF-ResNet50 using SGD with Momentum coefficient 0.9. We use cosine learning rate decay [Loshchilov and Hutter, 2016] and baseline pre-processing including flips and random crops [Szegedy et al., 2017]. We also apply stochastic depth with a drop rate of 0.1 [Huang et al., 2016] and dropout with a drop rate of 0.25 [Srivastava et al., 2014]. We tune the learning rate on a logarithmic grid spaced by factors of 2, performing a single training run at each learning rate.

In Figure 3, we plot the performance of both models in the large batch limit for a range of compute budgets. Note that since the number of unique images per batch now decreases as the augmentation multiplicity increases, larger multiplicities perform more parameter updates per epoch of training. We therefore provide the test accuracy achieved for a given epoch budget in figures a and c, as well as the test accuracy achieved within a given number of parameter updates in figures b and d. For clarity, since the batch size is fixed, the total number of gradient evaluations performed is proportional to the number of parameter updates. Considering first figures a and c, for both models large augmentation multiplicities achieve significantly higher test accuracy while requiring smaller epoch budgets. For instance on the ResNet-50, augmentation multiplicity 8 achieves 78.6% top-1 accuracy after 128 epochs, while augmentation multiplicity 1 achieves a peak accuracy of 77.3% after 512 epochs.

Remarkably, in figures b and d, we observe that moderately large augmentation multiplicities also achieve higher test accuracy than normal training ($n=1$) without requiring more parameter updates (and therefore without requiring more compute). For instance on the Wide-ResNet, augmentation multiplicity 1 achieves $72.1 \pm 0.1\%$ after 4×10^5 updates, while multiplicity 4 achieves $73.7 \pm 0.04\%$. Furthermore, large augmentation multiplicities benefit from additional parameter updates, achieving significantly higher peak accuracies, while the performance of normal training degrades rapidly.

In Figure 4, we provide a similar panel of figures, when training the same two models in the small batch limit. Considering first figures 4(a) and 4(c), we find on both CIFAR-100 and ImageNet that augmentation multiplicities larger than 1 still achieve higher test accuracy while also requiring fewer training epochs. On CIFAR-100, the benefits of augmentation multiplicity saturate for multiplicities $n \gtrsim 4$, while on ImageNet the peak test accuracy continues to rise for all multiplicities considered. We conclude that augmentation multiplicity is not only beneficial during large batch training [Hoffer et al., 2019], but also enhances generalization when the batch size is small. Meanwhile, in figure 4(b) we find that larger augmentation multiplicities do require more parameter updates to achieve superior performance for small batch sizes on CIFAR-100, while in figure 4(d) we find that larger augmentation multiplicities achieve superior test accuracy on ImageNet within a similar number of parameter updates. Taken together, figures 3 and 4 suggest that augmentation multiplicity consistently enhances the performance of residual networks in computer vision across a range of domains.

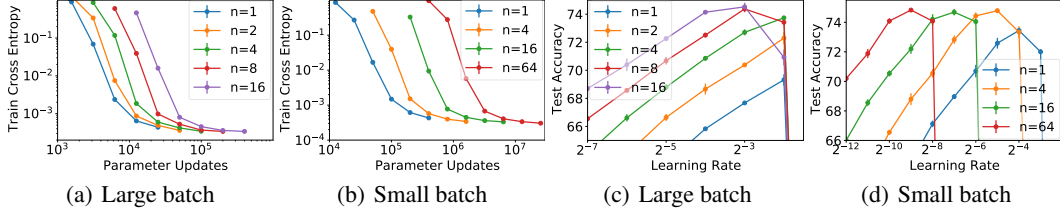
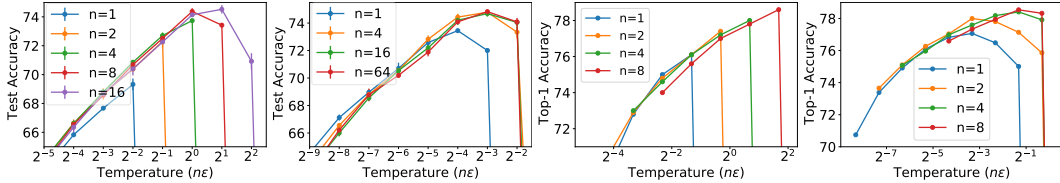


Figure 5: A 16-4 Wide-ResNet trained on CIFAR-100 at batch size 1024 and 64. Small augmentation multiplicities achieve lower training loss after a given number of parameter updates (a/b). For large batch sizes, large augmentation multiplicities achieve higher test accuracy at the same learning rate (c). For small batch sizes, large augmentation multiplicities require smaller learning rates (d).



(a) CIFAR-100/large batch (b) CIFAR-100/small batch (c) ImageNet/large batch (d) ImageNet/small batch

Figure 6: We plot the test accuracy accuracy at a range of ‘temperatures’ for a 16-4 Wide-ResNet on CIFAR-100 (a/b) and an NF-ResNet50 on ImageNet (c/d) after 128 epochs of training with both large and small batch sizes. We define the temperature as the product of the learning rate ϵ and the augmentation multiplicity n . Remarkably, in all four cases different augmentation multiplicities achieve similar performance when the temperature is small, however larger augmentation multiplicities are stable at higher temperatures, which enables them to achieve higher test accuracies overall.

4 Why do large augmentation multiplicities enhance generalization?

In Section 3, we demonstrated that augmentation multiplicities larger than 1 achieve higher test accuracy for both small and large batch training, despite containing fewer unique training examples in each minibatch. At first glance, this phenomenon is highly surprising. The gradients evaluated on different augmentations of the same image are correlated, while the gradients evaluated on independent training examples are not correlated [Hoffer et al., 2019]. Consequently if we maintain a fixed batch size but reduce the number of unique images in the minibatch, the overall variance in our estimate of the gradient will increase, which we might intuitively expect to degrade performance.

To show augmentation multiplicity only enhances test performance (for fixed batch sizes), we plot the cross entropy achieved on the training set after a given number of parameter updates when training the Wide-ResNet on CIFAR-100 at batch size 1024 in Figure 5(a) and batch size 64 in Figure 5(b). In both cases, smaller augmentation multiplicities achieve faster convergence on the training set.

We recall that when training with growing batches in Section 2, we observed that large augmentation multiplicities were stable at larger learning rates, which appeared to account for their superior test accuracy. To investigate whether a similar phenomenon arises when the batch size is fixed, we plot the test accuracy achieved at a range of learning rates when training the Wide-ResNet on CIFAR-100 for 128 epochs at batch size 1024 in Figure 5(c) and at batch size 64 in Figure 5(d). We observe different behaviour in the small and large batch regimes. For large batch training, large augmentation multiplicities achieve higher test accuracy at similar learning rates, while for small batch sizes large augmentation multiplicities achieve higher test accuracy but require smaller learning rates. In both cases, large augmentation multiplicities do not enable stable training at larger learning rates.

To explain these observations, we note that a large body of work has found that large learning rates have an implicit regularization benefit which enhances the test accuracy, and the strength of this regularization benefit is proportional to the ratio of the learning rate to the batch size [Jastrz bski et al., 2018, Li et al., 2019, Smith et al., 2021]. However prior empirical work has not distinguished whether reducing the batch size enhances the implicit regularization effect by reducing the number of unique examples in the minibatch, or whether it enhances the implicit regularization effect because it increases the variance in the minibatch gradient arising from the data augmentation procedure.

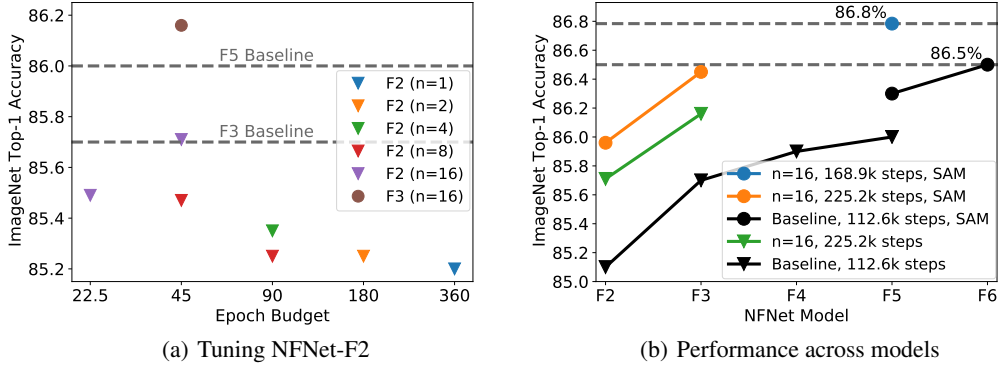


Figure 7: An evaluation of augmentation multiplicity on ImageNet using NFNets. (a) We consider a range of augmentation multiplicities on NFNets-F2 and NFNets-F3, trained at batch size 4096 without the SAM optimizer [Foret et al., 2021]. Larger augmentation multiplicities achieve higher top-1 accuracy and require fewer training epochs. For clarity, note that we define an epoch as a single pass through the training set. (b) We compare the performance achieved at augmentation multiplicity 16 to the original performance reported at augmentation multiplicity 1 by Brock et al. [2021b]. Circles denote models trained with SAM, while triangles denote models trained without SAM. Black points denote the original NFNets results reported by Brock et al. [2021b]. Our models reach substantially higher top-1 accuracy both with and without SAM. We achieve within 0.05% of the previous SOTA with an NFNets-F3, while our NFNets-F5 model sets a new SOTA without extra data of 86.8%.

We observed in Section 2 that reducing the variance arising from the data augmentation procedure increases the test accuracy. We therefore conclude that the implicit regularization benefit of SGD arises from the variance introduced by minibatching, not the variance introduced by data augmentation. On this basis, we predict that when using augmentation multiplicity, the generalization benefit will be governed by the ratio of the learning rate to the number of unique training examples in the batch, not the ratio of the learning rate to the batch size. When the number of unique examples in each minibatch is fixed (Section 2), this ratio is directly proportional to the learning rate. However, when the batch size is fixed, this ratio is proportional to the product of the learning rate and the augmentation multiplicity, which we define for clarity as the ‘temperature’ [Smith and Le, 2018, Park et al., 2019].

In Figure 6, we plot the test accuracy achieved after 128 epochs for both Wide-ResNet/CIFAR-100 and NF-ResNet50/ImageNet in both the small and large batch limits at a range of temperatures. Remarkably, we observe very similar behaviour in each plot. Different augmentation multiplicities achieve similar test accuracy when the temperature is small, but large augmentation multiplicities are stable at larger temperatures, and this enables them to achieve higher test accuracy overall. These figures suggest that large augmentation multiplicities achieve higher test accuracy because they suppress the noise in the gradient arising from the data augmentation procedure. This enables stable training at larger temperatures, which enhances the generalization benefit of finite learning rates.

We note however that, as observed in both Section 2 and Section 3, large augmentation multiplicities do achieve lower test accuracy for epoch budgets larger than the optimal epoch budget. This suggests that the variance in the gradient arising from data augmentation can help reduce over-fitting when models are over-trained. For completeness, we show in Appendix C that different augmentation multiplicities do not achieve similar test accuracy at the same temperature for large epoch budgets.

5 An empirical evaluation of augmentation multiplicity for NFNets

In Section 3, we showed that large augmentation multiplicities enhance generalization for both small and large batch training. In this section, we verify that these benefits continue to arise for highly performant, strongly regularized models. To achieve this goal, we evaluate the performance of augmentation multiplicity on the NFNets model family, recently proposed by Brock et al. [2021b]. NFNets comprise a family of models, denoted by NFNets-F x , where $x \in \{1, 2, 3, 4, 5, 6\}$. These models were designed such that it takes roughly twice as long to evaluate a gradient for F2 as for F1 on similar hardware, and similarly twice as long to evaluate a gradient for F3 as for F2, and so on.

Table 1: NFNet-F2 trained on ImageNet for a range of augmentation multiplicities, without the SAM optimizer, at batch size 4096. Large augmentation multiplicities achieve higher top-1 accuracy for the same number of parameter updates, and their performance improves further if we increase the compute budget. We also report the performance of NFNet-F3 trained for 225,200 updates at augmentation multiplicity 16. Results marked with an * are taken from Brock et al. [2021b]

	NFNet-F2 w/out SAM					NFNet-F3 w/out SAM	
Parameter updates:	Augmentation Multiplicity:					Augmentation Multiplicity:	
	1	2	4	8	16	1	16
112,600	85.20	85.25	85.35	85.47	85.49	85.7*	–
225,200	–	–	84.53	85.25	85.71	–	86.16

Table 2: NFNet-F3 and NFNet-F5, trained on ImageNet at augmentation multiplicity 16 with the SAM optimizer at batch size 4096. NFNet-F5 sets a new SOTA w/out extra data of 86.78% top-1 after 168,900 updates, while requiring a slightly smaller computation budget than the previous SOTA.

Augmentation Multiplicity 16	NFNet-F3 w/ SAM		NFNet-F5 w/ SAM	
Parameter Updates:	112,600	225,200	112,600	168,900
	85.76	86.45	86.54	86.78

NFNets are highly expressive, and consequently they benefit from extremely strong regularization and data augmentation, incorporating Dropout [Srivastava et al., 2014], Stochastic Depth [Huang et al., 2016], RandAugment [Cubuk et al., 2020], Mixup [Zhang et al., 2018] and Cutmix [Yun et al., 2019]. They are therefore ideally suited to evaluating the performance of large augmentation multiplicities.

Following the implementation of Brock et al. [2021b], we train each model variant with a batch size of 4096 using SGD with a momentum coefficient of 0.9, cosine annealing [Loshchilov and Hutter, 2016], and Adaptive Gradient Clipping (AGC). A moving average of the weights is stored during training and used to make predictions during inference [Szegedy et al., 2015]. We provide results both with and without Sharpness-Aware Minimization (SAM) [Foret et al., 2021], an optimization technique which enhances generalization but roughly doubles the time required to compute a gradient. Brock et al. [2021b] use learning rate $\epsilon = 1.6$, however we found $\epsilon = 0.8$ achieves higher top-1 accuracy for large augmentation multiplicities, which we adopt for all multiplicities $n > 1$. In the original study, all models were trained for 112,600 parameter updates (corresponding to 360 epochs for augmentation multiplicity 1). For all other details, we refer the reader to Brock et al. [2021b].

In Table 1, we provide a detailed evaluation of how augmentation multiplicity influences the performance of NFNet-F2, trained without SAM. Note that when applying augmentation multiplicities larger than 1, we take care to ensure that Mixup and CutMix are applied to different training inputs, and not different augmentations of the same image. We find that larger augmentation multiplicities achieve higher test accuracy, even under a fixed compute budget of 112,600 parameter updates, while augmentation multiplicity 16 continues to improve when the compute budget is increased to 225,200 updates. As we show in Figure 7(a), these results indicate that large augmentation multiplicities require an order of magnitude fewer training epochs to achieve similar or superior top-1 accuracies. For clarity, we emphasize that we use ‘epoch’ to denote a full pass through the training set, and that large augmentation multiplicities still require similar numbers of parameter updates. Intriguingly however, our results demonstrate we could dramatically reduce the computational cost of training large vision models if we could reduce the variance arising from the data augmentation procedure.

Finally, in Table 2 we report the performance of NFNet-F3 and NFNet-F5 when trained with SAM [Foret et al., 2021] at augmentation multiplicity 16. Our NFNet-F3 achieves 86.45% top-1 accuracy after 225,200 updates, within 0.05% of the previous SOTA of 86.5% achieved by an NFNet-F6 with SAM after 112,600 updates [Brock et al., 2021b]. Note however that since the NFNet-F3 requires roughly 8x less time to evaluate a gradient, it achieves this result with roughly 4x less total compute, and is also significantly faster to evaluate at inference. After applying augmentation multiplicity, our NFNet-F5 with SAM achieves a new SOTA w/o extra data of 86.78% after 168,900 updates. For clarity, we plot a range of results with and without SAM in Figure 7(b). Large augmentation multiplicities consistently outperform the baseline accuracies reported by Brock et al. [2021b].

6 Discussion

Our analysis suggests that the benefits of data augmentation when training deep ResNets [He et al., 2016] arise because the augmentation procedure introduces a bias in the mini-batch gradients. Data augmentation also introduces variance into the gradient estimate, but after tuning the epoch budget we found that this variance was detrimental to final performance, although it did help prevent overfitting if models were over-trained. Intriguingly, our study was inspired primarily by a recent study of the origin of the regularization benefits of dropout [Wei et al., 2020]. Like data augmentation, dropout introduces both bias and variance into the minibatch gradients. However Wei et al. [2020] found that in LSTMs both the bias and the variance introduced by dropout contribute to generalization. For completeness, we investigate the roles of bias and variance in dropout for Wide-ResNets in appendix E. We do not observe a significant generalization benefit from variance in these experiments.

We have shown that large augmentation multiplicities achieve higher test accuracy, both when the batch size is proportional to the augmentation multiplicity, and when the batch size is fixed, such that the number of unique images in each minibatch decreases as the augmentation multiplicity increases. A natural question raised by this observation is whether the benefits of augmentation multiplicity arise because we sample multiple augmentations of the same image in the same minibatch, or whether it is sufficient to resample different augmentations of the same unique images in neighbouring minibatches. We briefly compare these two schemes empirically in appendix D, where we find that, while both implementations achieve higher test accuracy than standard training, the benefits of augmentation multiplicity are most significant when we sample multiple augmentations per unique image inside the same minibatch. In particular, this scheme achieves superior performance for large multiplicities.

An inherent limitation of augmentation multiplicity is that it can only be used for networks trained using data augmentation. However the use of data augmentation in deep learning is extremely common, and in particular we note that it is a core component of self-supervised learning [Chen et al., 2020, He et al., 2020, Grill et al., 2020]. An additional limitation of our study is that we only consider residual networks on computer vision benchmarks. We leave it to future work to establish whether the benefits of augmentation multiplicity also arise for other model families and data modalities.

7 Conclusion

We provide an empirical study of how the augmentation multiplicity (the number of samples drawn from the augmentation operation per unique image in each minibatch) influences test accuracy when training deep residual networks. Remarkably, we find that augmentation multiplicities greater than 1 consistently achieve higher test accuracy, often without requiring larger computation budgets. These benefits are particularly significant during large batch training but also arise when the batch size is small. Using an augmentation multiplicity of 16, we set a new ImageNet SOTA of 86.8% top-1 accuracy after just 34 epochs of training (168,900 parameter updates at batch size 4096) with an NFNet-F5 using the SAM optimizer. Our study suggests practitioners should consider choosing large augmentation multiplicities as the default when training deep neural networks for computer vision.

Acknowledgements

We thank Yee Whye Teh, Karen Simonyan, Zahra Ahmed and Hyunjik Kim for helpful advice, and Matthias Bauer for feedback on an earlier draft of the manuscript.

References

- Andrew Brock, Soham De, and Samuel L Smith. Characterizing signal propagation to close the performance gap in unnormalized resnets. In *International Conference on Learning Representations*, 2021a. URL <https://openreview.net/forum?id=IX3Nnir2omJ>.
- Andrew Brock, Soham De, Samuel L Smith, and Karen Simonyan. High-performance large-scale image recognition without normalization. *arXiv preprint arXiv:2102.06171*, 2021b.
- Pratik Chaudhari and Stefano Soatto. Stochastic gradient descent performs variational inference, converges to limit cycles for deep networks. In *2018 Information Theory and Applications Workshop (ITA)*, pages 1–10. IEEE, 2018.
- Ting Chen, Simon Kornblith, Mohammad Norouzi, and Geoffrey Hinton. A simple framework for contrastive learning of visual representations. In *International conference on machine learning*, pages 1597–1607. PMLR, 2020.
- Dami Choi, Alexandre Passos, Christopher J Shallue, and George E Dahl. Faster neural network training with data echoing. *arXiv preprint arXiv:1907.05550*, 2019.
- Ekin D Cubuk, Barret Zoph, Jonathon Shlens, and Quoc V Le. Randaugment: Practical automated data augmentation with a reduced search space. In *Proceedings of the IEEE/CVF Conference on Computer Vision and Pattern Recognition Workshops*, pages 702–703, 2020.
- Soham De and Sam Smith. Batch normalization biases residual blocks towards the identity function in deep networks. *Advances in Neural Information Processing Systems*, 33, 2020.
- Alexey Dosovitskiy, Lucas Beyer, Alexander Kolesnikov, Dirk Weissenborn, Xiaohua Zhai, Thomas Unterthiner, Mostafa Dehghani, Matthias Minderer, Georg Heigold, Sylvain Gelly, et al. An image is worth 16x16 words: Transformers for image recognition at scale. *arXiv preprint arXiv:2010.11929*, 2020.
- Pierre Foret, Ariel Kleiner, Hossein Mobahi, and Behnam Neyshabur. Sharpness-aware minimization for efficiently improving generalization. In *International Conference on Learning Representations*, 2021. URL <https://openreview.net/forum?id=6Tm1mposlrM>.
- Priya Goyal, Piotr Dollár, Ross Girshick, Pieter Noordhuis, Lukasz Wesolowski, Aapo Kyrola, Andrew Tulloch, Yangqing Jia, and Kaiming He. Accurate, Large Minibatch SGD: Training Imagenet in 1 Hour. *arXiv preprint arXiv:1706.02677*, 2017.
- Jean-Bastien Grill, Florian Strub, Florent Altché, Corentin Tallec, Pierre Richemond, Elena Buchatskaya, Carl Doersch, Bernardo Avila Pires, Zhaohan Guo, Mohammad Gheshlaghi Azar, Bilal Piot, Koray Kavukcuoglu, Remi Munos, and Michal Valko. Bootstrap your own latent - a new approach to self-supervised learning. In *Advances in Neural Information Processing Systems*, volume 33, pages 21271–21284, 2020.
- Kaiming He, Xiangyu Zhang, Shaoqing Ren, and Jian Sun. Identity mappings in deep residual networks. In *European conference on computer vision*, pages 630–645. Springer, 2016.
- Kaiming He, Haoqi Fan, Yuxin Wu, Saining Xie, and Ross Girshick. Momentum contrast for unsupervised visual representation learning. In *Proceedings of the IEEE/CVF Conference on Computer Vision and Pattern Recognition*, pages 9729–9738, 2020.
- Elad Hoffer, Itay Hubara, and Daniel Soudry. Train longer, generalize better: closing the generalization gap in large batch training of neural networks. In *Advances in Neural Information Processing Systems*, pages 1731–1741, 2017.
- Elad Hoffer, Tal Ben-Nun, Itay Hubara, Niv Giladi, Torsten Hoeffler, and Daniel Soudry. Augment your batch: better training with larger batches. *arXiv preprint arXiv:1901.09335*, 2019.
- Gao Huang, Yu Sun, Zhuang Liu, Daniel Sedra, and Kilian Q Weinberger. Deep networks with stochastic depth. In *European conference on computer vision*, pages 646–661. Springer, 2016.

- Stanisław Jastrzębski, Zachary Kenton, Devansh Arpit, Nicolas Ballas, Asja Fischer, Yoshua Bengio, and Amos Storkey. Three Factors Influencing Minima in SGD. In *Artificial Neural Networks and Machine Learning, ICANN*, 2018.
- Nitish Shirish Keskar, Dheevatsa Mudigere, Jorge Nocedal, Mikhail Smelyanskiy, and Ping Tak Peter Tang. On large-batch training for deep learning: Generalization gap and sharp minima. In *International Conference on Learning Representations, ICLR*, 2017.
- Alex Krizhevsky, Geoffrey Hinton, et al. Learning multiple layers of features from tiny images. *Technical Report*, 2009.
- Yuanzhi Li, Colin Wei, and Tengyu Ma. Towards explaining the regularization effect of initial large learning rate in training neural networks. In *Advances in Neural Information Processing Systems*, pages 11669–11680, 2019.
- Ilya Loshchilov and Frank Hutter. Sgdr: Stochastic gradient descent with warm restarts. *arXiv preprint arXiv:1608.03983*, 2016.
- Siyuan Ma, Raef Bassily, and Mikhail Belkin. The power of interpolation: Understanding the effectiveness of SGD in modern over-parametrized learning. In *Proceedings of the 35th International Conference on Machine Learning, ICML*, 2018.
- Stephan Mandt, Matthew D Hoffman, and David M Blei. Stochastic gradient descent as approximate bayesian inference. *The Journal of Machine Learning Research*, 18(1):4873–4907, 2017.
- Daniel Park, Jascha Sohl-Dickstein, Quoc Le, and Samuel Smith. The effect of network width on stochastic gradient descent and generalization: an empirical study. In *International Conference on Machine Learning*, pages 5042–5051, 2019.
- Olga Russakovsky, Jia Deng, Hao Su, Jonathan Krause, Sanjeev Satheesh, Sean Ma, Zhiheng Huang, Andrej Karpathy, Aditya Khosla, Michael Bernstein, Alexander C. Berg, and Li Fei-Fei. ImageNet Large Scale Visual Recognition Challenge. *International Journal of Computer Vision (IJCV)*, 115(3):211–252, 2015. doi: 10.1007/s11263-015-0816-y.
- Connor Shorten and Taghi M Khoshgoftaar. A survey on image data augmentation for deep learning. *Journal of Big Data*, 6(1):1–48, 2019.
- Samuel L Smith and Quoc V Le. A bayesian perspective on generalization and stochastic gradient descent. In *International Conference on Learning Representations*, 2018.
- Samuel L Smith, Erich Elsen, and Soham De. On the generalization benefit of noise in stochastic gradient descent. In *International Conference on Machine Learning*, 2020.
- Samuel L Smith, Benoit Dherin, David Barrett, and Soham De. On the origin of implicit regularization in stochastic gradient descent. In *International Conference on Learning Representations*, 2021. URL https://openreview.net/forum?id=rq_Qr0c1Hyo.
- Nitish Srivastava, Geoffrey Hinton, Alex Krizhevsky, Ilya Sutskever, and Ruslan Salakhutdinov. Dropout: a simple way to prevent neural networks from overfitting. *The journal of machine learning research*, 15(1):1929–1958, 2014.
- Christian Szegedy, Wei Liu, Yangqing Jia, Pierre Sermanet, Scott Reed, Dragomir Anguelov, Dumitru Erhan, Vincent Vanhoucke, and Andrew Rabinovich. Going deeper with convolutions. In *Proceedings of the IEEE conference on computer vision and pattern recognition*, pages 1–9, 2015.
- Christian Szegedy, Vincent Vanhoucke, Sergey Ioffe, Jon Shlens, and Zbigniew Wojna. Rethinking the inception architecture for computer vision. In *Proceedings of the IEEE conference on computer vision and pattern recognition*, pages 2818–2826, 2016.
- Christian Szegedy, Sergey Ioffe, Vincent Vanhoucke, and Alexander Alemi. Inception-v4, inception-resnet and the impact of residual connections on learning. In *Proceedings of the AAAI Conference on Artificial Intelligence*, volume 31, 2017.
- Hugo Touvron, Matthieu Cord, Alexandre Sablayrolles, Gabriel Synnaeve, and Hervé Jégou. Going deeper with image transformers. *arXiv preprint arXiv:2103.17239*, 2021.

- Colin Wei, Sham Kakade, and Tengyu Ma. The implicit and explicit regularization effects of dropout. In *International Conference on Machine Learning*, pages 10181–10192. PMLR, 2020.
- Sangdoon Yun, Dongyoon Han, Seong Joon Oh, Sanghyuk Chun, Junsuk Choe, and Youngjoon Yoo. Cutmix: Regularization strategy to train strong classifiers with localizable features. In *Proceedings of the IEEE/CVF International Conference on Computer Vision*, pages 6023–6032, 2019.
- Sergey Zagoruyko and Nikos Komodakis. Wide residual networks. In *Proceedings of the British Machine Vision Conference (BMVC)*, pages 87.1–87.12, September 2016.
- Guodong Zhang, Lala Li, Zachary Nado, James Martens, Sushant Sachdeva, George E. Dahl, Christopher J. Shallue, and Roger B. Grosse. Which Algorithmic Choices Matter at Which Batch Sizes? Insights From a Noisy Quadratic Model. In *Advances in Neural Information Processing Systems*, 2019.
- Hongyi Zhang, Moustapha Cisse, Yann N. Dauphin, and David Lopez-Paz. mixup: Beyond empirical risk minimization. In *International Conference on Learning Representations*, 2018. URL <https://openreview.net/forum?id=r1Ddp1-Rb>.

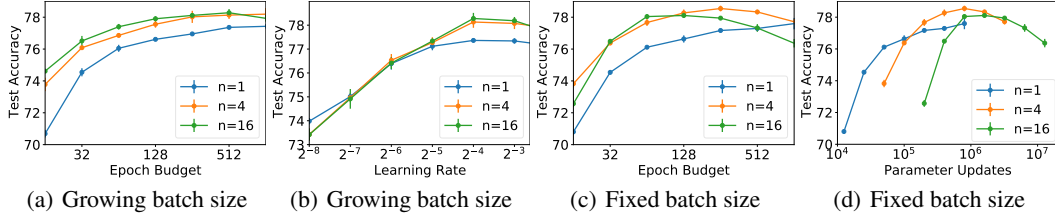


Figure 8: A 16-4 Wide-ResNet trained on CIFAR-100 with batch normalization and augmentation multiplicity. In figures (a) and (b), we hold the number of unique images in each minibatch fixed, such that the batch size grows with augmentation multiplicity. In figures (c) and (d) we hold the batch size fixed, such that the number of unique images in each minibatch shrinks as the augmentation multiplicity increases. In both cases, augmentation multiplicities $n > 1$ achieve higher test accuracy.

A Augmentation multiplicity and batch normalization

The performance of batch normalized models is known to depend strongly on the “ghost batch size” [Hoffer et al., 2017], the number of examples over which we estimate the batch statistics. The optimal value of this ghost batch size will depend on the augmentation multiplicity, and consequently it is challenging to provide a rigorous evaluation of augmentation multiplicity in batch normalized models. We therefore focus on performant networks which do not apply batch normalization in the main text.

However, to verify that our insights carry over to batch normalized networks, we provide a limited evaluation in Figure 8. We consider a batch normalized 16-4 Wide-ResNet trained on CIFAR-100, following the training protocol described in section 2. In Figures 8(a) and 8(b), we fixed the number of unique images in each minibatch equal to 64, such that the batch size $B = 64n$ grows as the augmentation multiplicity n increases. Meanwhile in Figures 8(c) and 8(d) we fix the total batch size $B = 64$, such that the number of unique images in each batch decreases as the augmentation multiplicity decreases. In all experiments, the ghost batch size is set equal to the full minibatch. Consequently in Figures 8(a) and 8(b) the ghost batch size contains a fixed number of unique images, while in Figures 8(c) and 8(d) the ghost batch size contains a fixed number of augmented images.

Considering first Figure 8(a), in the growing batch regime, larger augmentation multiplicities achieve substantially higher test accuracy across a range of epoch budgets. Recall that at each epoch budget, we tune the learning rate on a logarithmic grid spaced by factors of 2, and we plot the mean test accuracy of the best 5 out of 7 training runs. In Figure 8(b) we plot the performance achieved across a range of learning rates for a compute budget of 512 epochs. As observed in the main text, we observe that large augmentation multiplicities achieve superior performance with large learning rates.

Now considering Figure 8(c), large augmentation multiplicities also achieve superior performance after a fixed number of training epochs when the total batch size is fixed, although the performance of large augmentation multiplicities degrades for large epoch budgets. Finally, we verify in Figure 8(d) that large augmentation multiplicities achieve superior test accuracy for a given number of parameter updates (equivalent to the total compute budget used). Note however that augmentation multiplicity 16 achieves lower peak test accuracy than multiplicity 4. We speculate that this occurs because there are too few unique training images in the minibatch to estimate the batch statistics reliably.

B Additional results with growing batch sizes

In this section, we provide additional results for the setting where the number of unique images in each batch is fixed, such that the batch size grows with the augmentation multiplicity. We consider an NF-ResNet-50 [Brock et al., 2021a] trained on ImageNet. Similar to Brock et al. [2021a], we train our models using SGD with Nesterov’s Momentum and use standard baseline preprocessing of the input images: sampling and resizing distorted bounding boxes to take random crops, along with random horizontal flips. We use a cosine annealing of the learning rate [Loshchilov and Hutter, 2016]. No learning rate warmup was used. We also use additional regularization in the form of weight decay with a coefficient of $5e-5$, label smoothing with a coefficient of 0.1 [Szegedy et al., 2016], stochastic

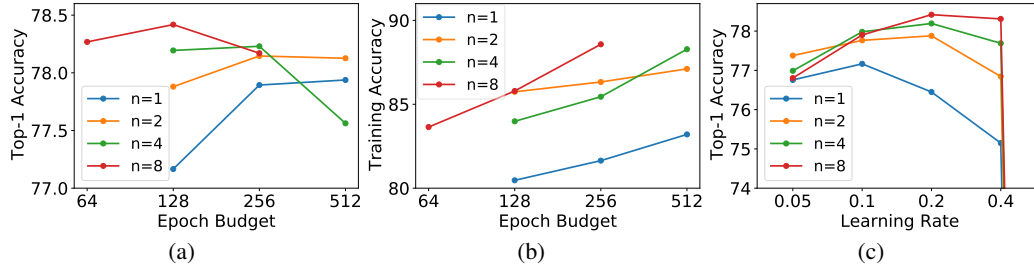


Figure 9: Results with a NF-ResNet-50 [Brock et al., 2021a] on ImageNet. The number of unique images per batch is fixed, such that the batch size grows as the augmentation multiplicity n increases. (a) Test accuracies at optimal learning rates for a range of epoch budgets. Large augmentation multiplicities achieve higher overall test accuracies, and also require fewer training epochs. (b) The training cross entropy for a range of epoch budgets. In this growing batch setting, large augmentation multiplicities achieve higher training accuracy. (c) The test accuracy at a range of learning rates for a compute budget of 128 epochs. Different multiplicities achieve similar test accuracy when the learning rate is small, but large multiplicities achieve higher test accuracy with large learning rates.

depth with a rate of 0.1 [Huang et al., 2016], and Dropout [Srivastava et al., 2014] before the final linear layer with a drop probability of 0.25. We perform a single training run at each learning rate.

We draw 256 unique inputs in each minibatch, such that the total batch size $B = 256n$ grows with the augmentation multiplicity n . As in Section 2, this ensures that the variance from data augmentation decreases as the augmentation multiplicity rises, while the variance arising from sampling minibatches from the training dataset does not change as the augmentation multiplicity rises.

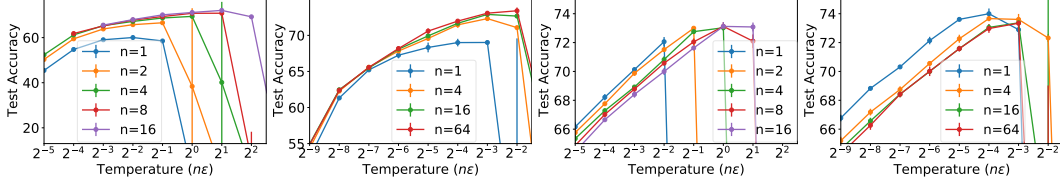
In Figure 9(a), we plot the top-1 accuracy for a range of augmentation multiplicities and epoch budgets. Note that we independently tune the learning rate on a logarithmic grid spaced by factors of 2 for each combination of epoch budget and augmentation multiplicity. As in Section 2, we find that large augmentation multiplicities achieve higher top-1 accuracies. For instance, an augmentation multiplicity of 8 achieves a peak top-1 accuracy of 78.4% after 128 epochs, whereas normal training (augmentation multiplicity 1) achieves a peak top-1 accuracy of 77.9% after 512 epochs. This strengthens our claim that the variance arising from data augmentation can harm generalization, and that the benefits of data augmentation arises from the bias introduced in the gradient.

In Figure 9(b), we plot the training accuracy at the learning rate in our grid that maximizes the training accuracy, and we show that large augmentation multiplicities also achieve higher training accuracies in this growing batch setting. This is similar to our observations in Section 2. Note that in these experiments, we evaluate the training accuracy on the minibatch used, not the full dataset.

Finally in Figure 9(c), we plot how the top-1 accuracy depends on the learning rate for different augmentation multiplicities when the epoch budget is 128 (which is the optimal epoch budget for large augmentation multiplicities). Similar to Section 2, we find that different augmentation multiplicities achieve similar top-1 accuracy when the learning rate is small, but that large augmentation multiplicities achieve higher top-1 accuracy when the learning rate is large.

C The dependence on the temperature for large epoch budgets

We showed in Section 4 that when the batch size is fixed, different augmentation multiplicities achieve similar test accuracy for moderate epoch budgets at small ‘temperatures’, which we define as the product of the augmentation multiplicity n and the learning rate ϵ , while large augmentation multiplicities achieve higher test accuracy for large temperatures. However we also observed that for large epoch budgets (when models are over-trained), small augmentation multiplicities can reduce overfitting. To explore this further, in Figure 10 we show how the test accuracy depends on the temperature for both small and large epoch budgets on our 16-4 Wide-ResNet/CIFAR-100. We find that at small epoch budgets, different augmentation multiplicities achieve similar test accuracy when the temperature is small, as observed for moderate epoch budgets in Section 4, while for large epoch budgets, small augmentation multiplicities achieve higher test accuracy at a given temperature, verifying that small augmentation multiplicities can help prevent overfitting in over-trained models.



(a) Large batch/32 epochs (b) Small batch/32 epochs (c) Large batch/512 epochs (d) Small batch/512 epochs

Figure 10: A 16-4 Wide-ResNet trained on CIFAR-100 at two batch sizes, 1024 (large) and 64 (small). In (a)/(b) we exhibit how the test accuracy depends on the temperature, defined as the product of the augmentation multiplicity n and the learning rate ϵ , for a budget of 32 training epochs. For both batch sizes, we find that the test accuracy is determined by the temperature for small epoch budgets when the temperature is also small, while large augmentation multiplicities achieve higher test accuracy for large temperatures. Meanwhile in (c)/(d), we show that small augmentation multiplicities achieve higher test accuracy at a given temperature when the epoch budget is large (512 training epochs).

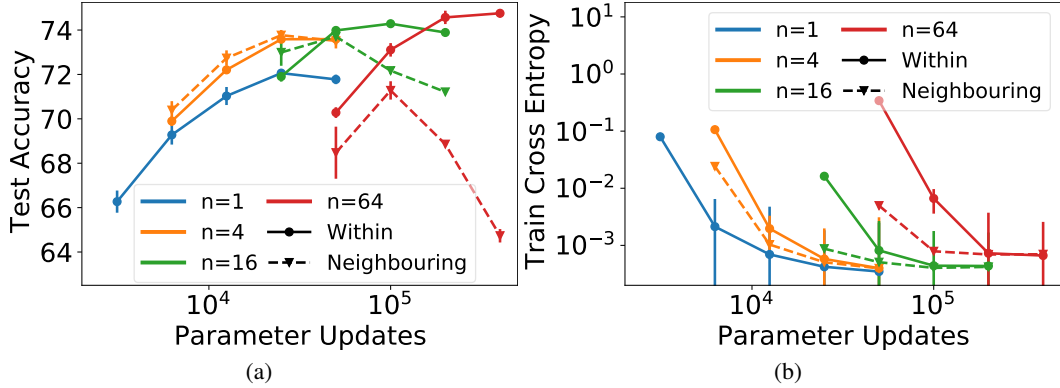


Figure 11: A 16-4 Wide-ResNet trained on CIFAR-100 with a fixed batch size of 1024. Solid lines (“within”) denote the default implementation of augmentation multiplicity, whereby we sample n augmentations per image within each minibatch (reducing the number of unique images per batch). Meanwhile dashed lines (“neighbouring”) denote an alternative scheme, whereby we only sample a single augmentation per image in each minibatch, but we resample the same training examples in n neighbouring minibatches (with different data augmentations). (a) We find that the neighbouring scheme can also enhance generalization for moderate multiplicities, however it performs poorly when the multiplicity is large. (b) The “neighbouring” scheme also achieves slightly lower training losses.

D Do multiple augmentations need to occur within the same minibatch?

In the main text, we analysed a single version of augmentation multiplicity. In this default implementation, we draw n augmentations of each unique image *within the same minibatch*. When the batch size is fixed, this implies the number of unique images per batch decreases as the augmentation multiplicity increases. In Figure 11 we compare this default implementation (which we refer to as “within”) to an alternative scheme, whereby we only sample a single augmentation per unique image in any single minibatch, but we sample the same set of unique images in n neighbouring minibatches. For clarity, these minibatches contain the same unique images but we draw different augmentations of each image in each adjacent minibatch. We refer to this alternative scheme as “neighbouring”.

Normal training (augmentation multiplicity 1) is shown in blue, the default implementation of augmentation multiplicity (“within”) is shown with full lines, and the alternative implementation (“neighbouring”) is shown with dashed lines. For moderate multiplicities, both implementations enhance the test accuracy, as shown in Figure 11(a). However for large augmentation multiplicities, the default implementation (“within”) continues to enhance generalization, while the performance of the alternative scheme (“neighbouring”) begins to degrade. We therefore conclude that to maximize the benefits of augmentation multiplicity, one should adopt the default implementation (“within”), placing multiple augmentations of the same image inside the same minibatch.

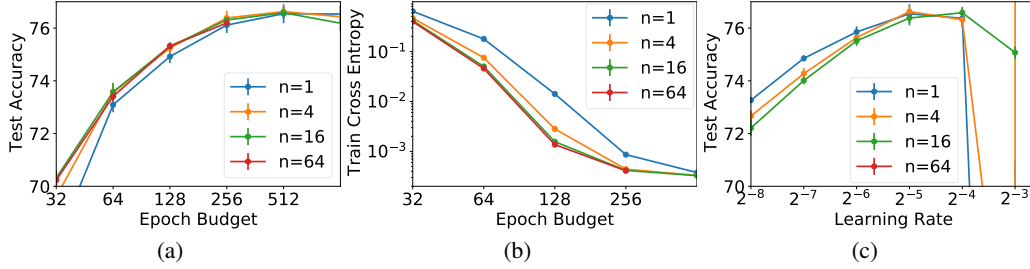


Figure 12: Results with a 16-4 Wide-ResNet on CIFAR-100, trained using dropout with a drop probability of 0.4. The number of unique images in each batch is fixed at 64, and we evaluate the performance at augmentation multiplicity 1. However we average each gradient across n models generated from n different samples of the dropout mask. In figure (a), we find that the test accuracy does not depend strongly on the number of samples of the dropout mask, which suggests that the benefits of dropout in this network arise from the bias introduced in the gradient, not the variance. In figure (b) we show that large numbers of samples minimize the training loss more quickly. Finally in figure (c) we provide the test accuracy achieved for a range of learning rates after 512 epochs.

E Bias and variance in dropout

Dropout [Srivastava et al., 2014] is a widely used regularization technique in deep learning. For each minibatch gradient evaluation, a random boolean mask is sampled which covers the output activations of a chosen layer of the network, such that any output unit (and its connections) is dropped with a specified drop probability. The purpose of dropout is to force the network to learn redundant representations, thus discouraging overfitting and enhancing generalization.

Like data augmentation, dropout has two influences on the gradient distribution. First, it changes the expected value of the gradient, introducing bias. Second, since we typically only sample a single dropout mask, dropout also introduces a source of variance. The roles of these two effects was studied by Wei et al. [2020], who refer to the bias and variance as the implicit and explicit regularization effects respectively. To disentangle the role of bias and variance, they take an average of n gradients evaluated for n different random dropout masks before taking each optimization step. The larger the n , the lower the variance arising from the stochasticity of sampling a dropout mask, while the bias remains unchanged. The authors found that both the bias and the variance arising from dropout enhance generalization in LSTMs. Note that by contrast, we found that the variance arising from the data augmentation procedure harms generalization for ResNets trained on CIFAR-100 and ImageNet.

We replicate the empirical analysis of Wei et al. [2020] for a 16-4 Wide-ResNet trained on CIFAR-100 in Figure 12. We apply dropout on the final linear layer of the network with drop probability 0.4, averaging each gradient over n samples of the dropout mask. Note that we average the gradient across different dropout masks but with the same augmentations of the input (i.e., the augmentation multiplicity is set to 1 throughout). We find that networks trained with dropout achieve higher test accuracy, while also requiring larger epoch budgets (see Figure 4(a) for an equivalent network trained without dropout at a range of augmentation multiplicities). However reducing the dropout variance by averaging the gradient across multiple masks does not appear to substantially enhance test accuracy, suggesting that the benefits of dropout in this network primarily arise from the bias in the gradient.